

5. A case study: the Aneurisk project

Aneurisk project

Sangalli, Vantini, Secchi, Veneziani 2009 JASA

A CONJECTURE

The pathogenesis of cerebral aneurysms is conditioned by the geometry of the cerebral vessels through its effects on blood fluid dynamics

SIEMENS



ANEURISK



Laboratory of Biological Structure Mechanics
Department of Structural Engineering



Azienda Ospedaliera
Ospedale Niguarda Ca'Granda



ISTITUTO DI
RICERCHE FARMACOLOGICHE



UNIVERSITÀ
DEGLI STUDI
DI MILANO

Statistics
Computer fluid dynamics

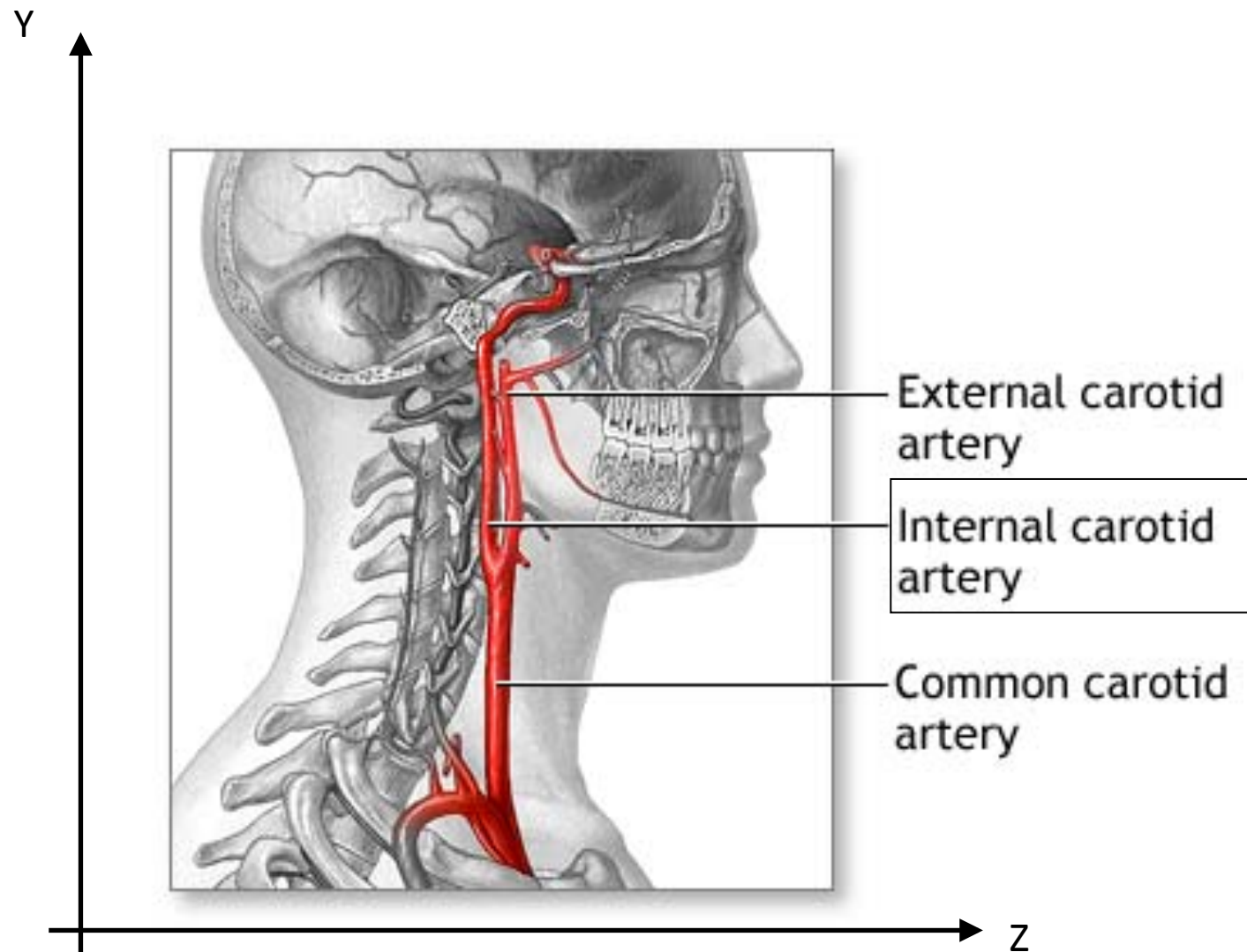
Structure Mechanics

Neuroradiology

Image Reconstruction

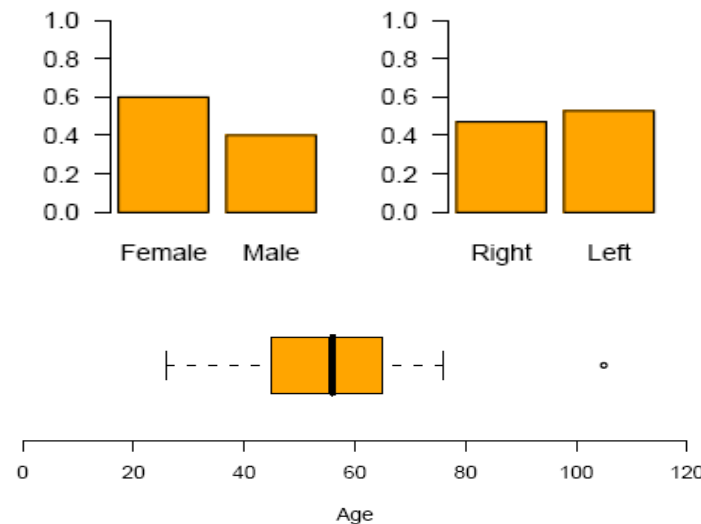
Neurosurgery

Aneurisk project



Data: 3D-angiographies

Observational Study conducted at Ospedale Ca' Granda Niguarda – Milano relative to 65 patients hospitalized from September 2002 to October 2005.



Upper group	Lower group	
Aneurysm at or after ICA biforc	Aneurysm before ICA biforc	No aneurysms
33	25	7



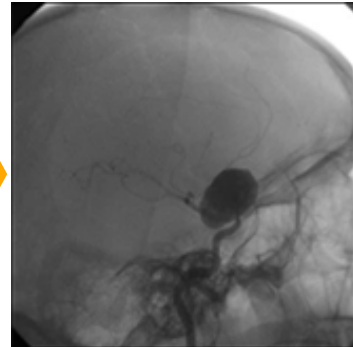
From X-rays to centerlines

Contrast Fluid Injections



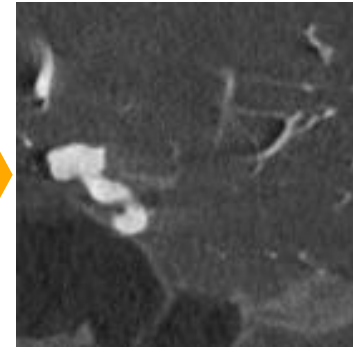
1

X-rays (one direction)



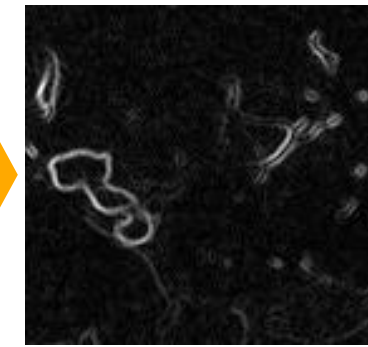
2

3d-array (one slice)



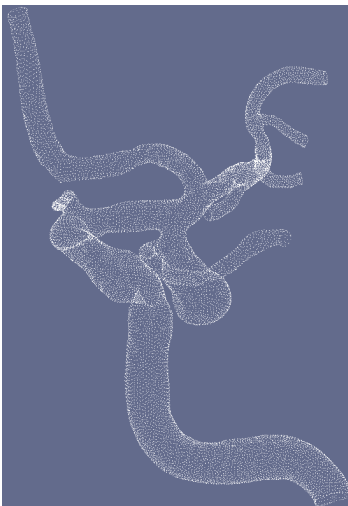
3

Gradient 3d-array (one slice)



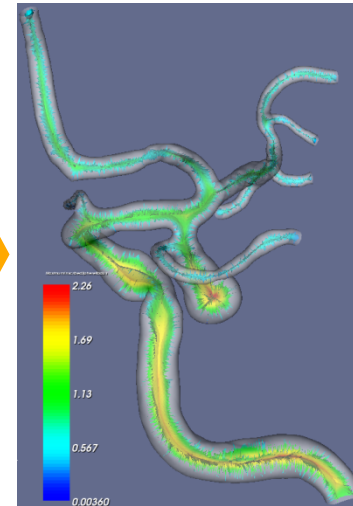
4

Surface Points



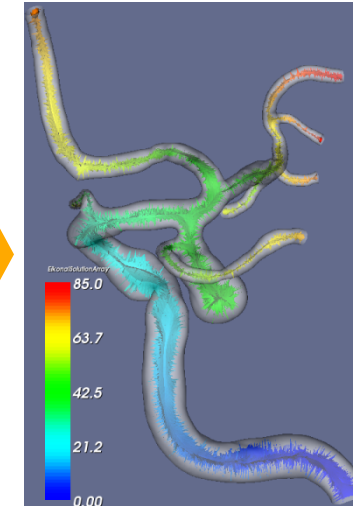
4

Voronoi Diagram



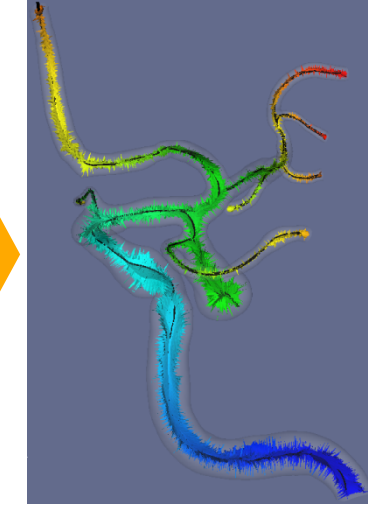
5

Eikonal Equation



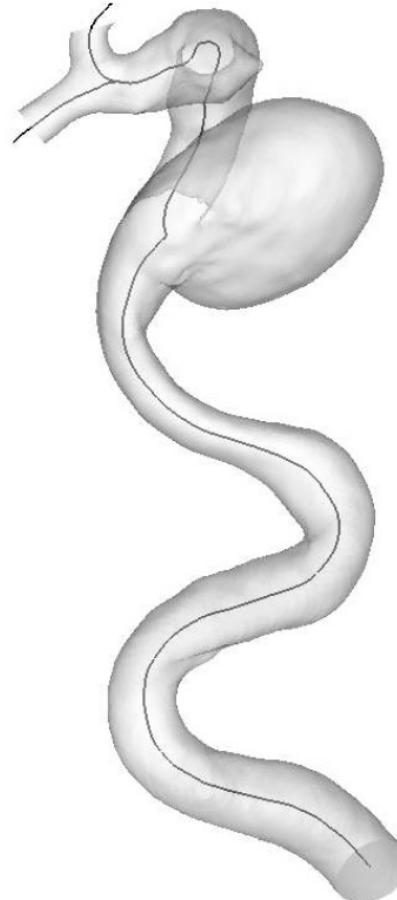
6

Centerline+MISR



7

Image Reconstruction (Antiga, Ene-lordache, Remuzzi, 2003)



Focus on Internal Carotid Artery (ICA)

For each patient i elicitation of 3-spatial coordinates of ICA centerline

$$\{(x_{ij}, y_{ij}, z_{ij}) : j = 1, \dots, n_i\}$$

and vessel radius

$$\{R_{ij} : j = 1, \dots, n_i\}$$

along a fine grid of points

$$(350 \leq n_i \leq 1380)$$

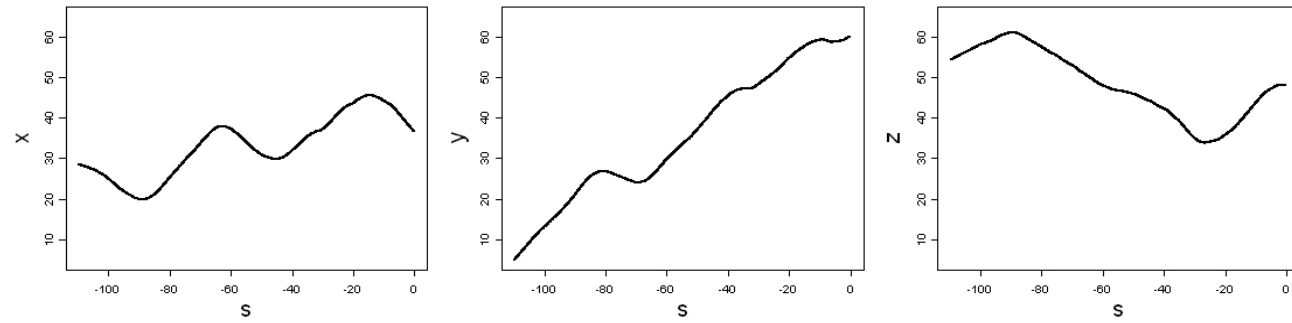
Approximate curvilinear α

Two geometric quantities that greatly influence the haemodynamics: vessel **radius** and **curvature** (curvature of its centerline)

$$s_{ij} - s_{ij-1} = -\sqrt{(x_{ij} - x_{ij-1})^2 + (y_{ij} - y_{ij-1})^2 + (z_{ij} - z_{ij-1})^2}, \quad j = 2, \dots, n_i$$

Centerline data

COORDINATES
PATIENT 1



Very high signal-to-noise ratio
Fine grid of observed points

Accurate curve estimation by 3D free-knot splines

(Sangalli, Secchi, Vantini, Veneziani, 2009)

$$\{b_{r,m}^{[k]}(s) : r = 1, \dots, m + n_k\}$$

b-spline basis system for the vector space
of splines of order m
with knot vector $\mathbf{k} = (k_1, \dots, k_{n_k})$

$$\hat{x}(s) = \sum_{r=1}^m \hat{\lambda}_r^{[x]} b_{r,m}^{[k]}(s)$$

$$\hat{y}(s) = \sum_{r=1}^m \hat{\lambda}_r^{[y]} b_{r,m}^{[k]}(s)$$

$$\hat{z}(s) = \sum_{r=1}^m \hat{\lambda}_r^{[z]} b_{r,m}^{[k]}(s)$$

FIND

by minimizing

$$\hat{n}_k, \hat{\mathbf{k}} = (\hat{k}_1(s), \dots, \hat{k}_{n_k}(s)), \hat{\lambda}^{[x]}, \hat{\lambda}^{[y]}, \hat{\lambda}^{[z]}$$

$$\sum_{j=1}^n \left(x_j - \sum_{r=1}^{m+n_k} \lambda_r^{[x]} b_{r,m}^{[k]}(s_j) \right)^2 + \sum_{j=1}^n \left(y_j - \sum_{r=1}^{m+n_k} \lambda_r^{[y]} b_{r,m}^{[k]}(s_j) \right)^2 + \sum_{j=1}^n \left(z_j - \sum_{r=1}^{m+n_k} \lambda_r^{[z]} b_{r,m}^{[k]}(s_j) \right)^2 + \mathcal{C}(m + n_k)$$

through a generalization of Zhou-Shen algorithm (*Zhou-Shen, JASA, 2001*)

FIX

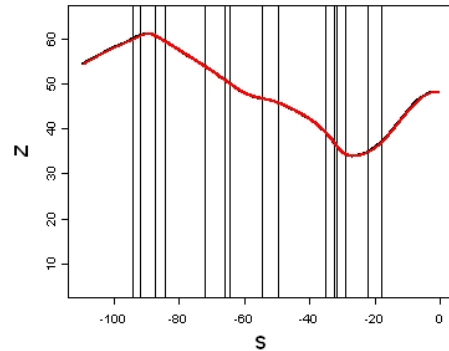
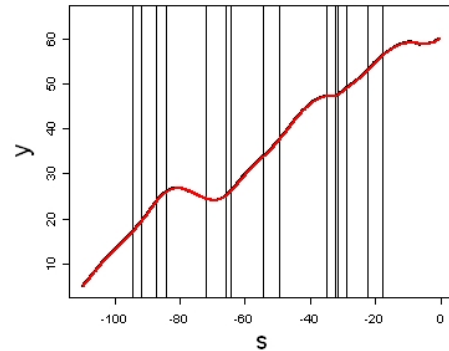
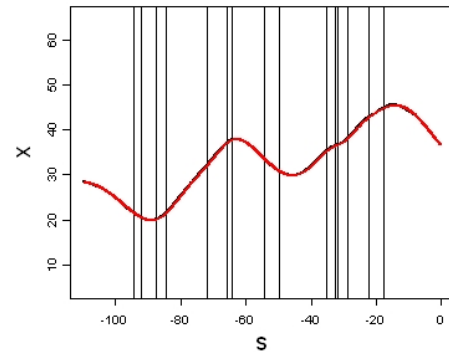
$$m = 5$$

to obtain smooth estimates of the curvature (function of second derivative)

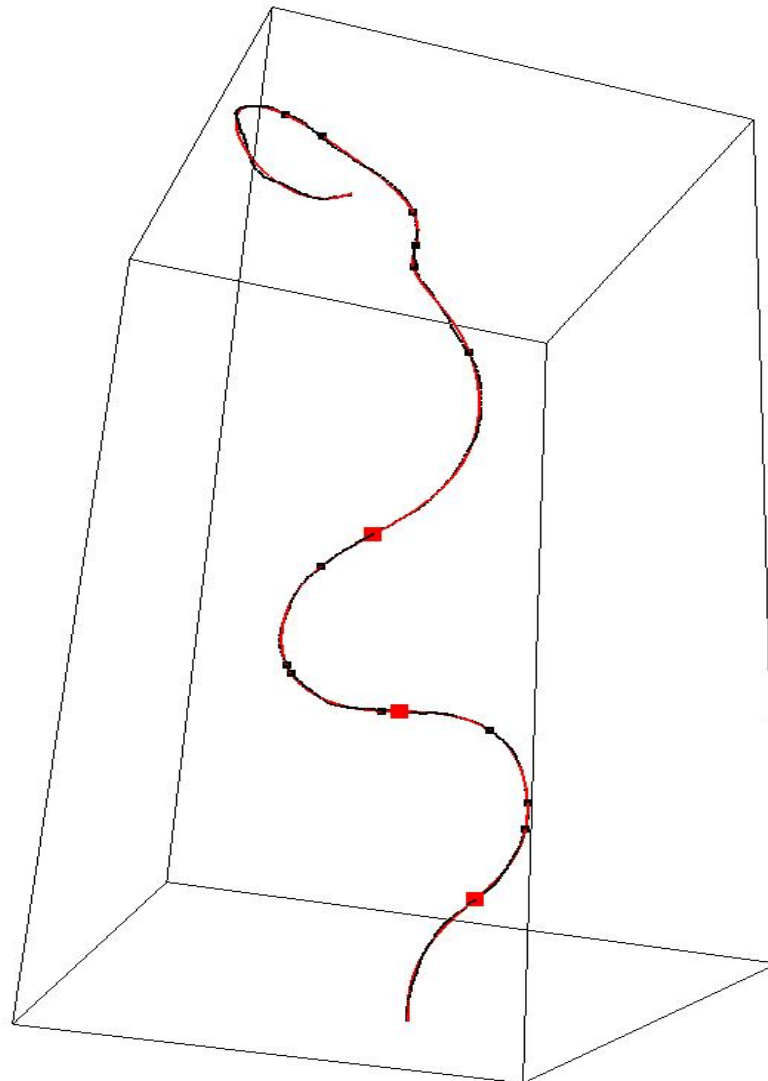
Accurate curve estimation by 3D free-knot splines

(Sangalli, Secchi, Vantini, Veneziani, 2009)

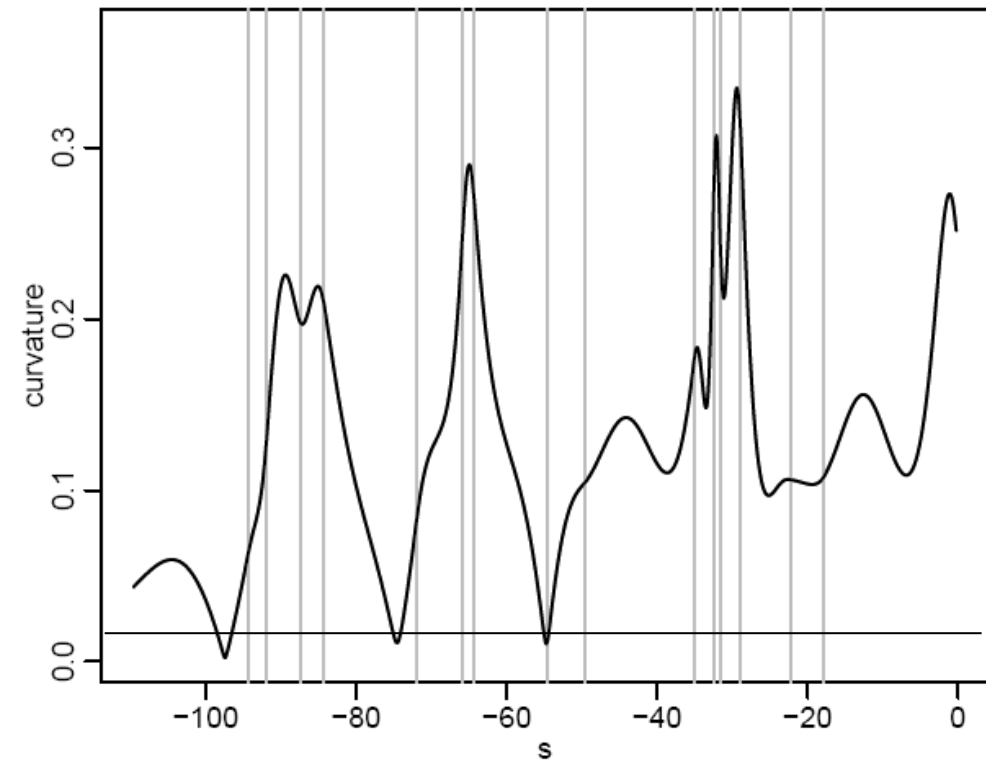
Curve estimate



Derivatives of splines are still splines with the same knot vector and coefficients directly computed from the coefficients of the original spline



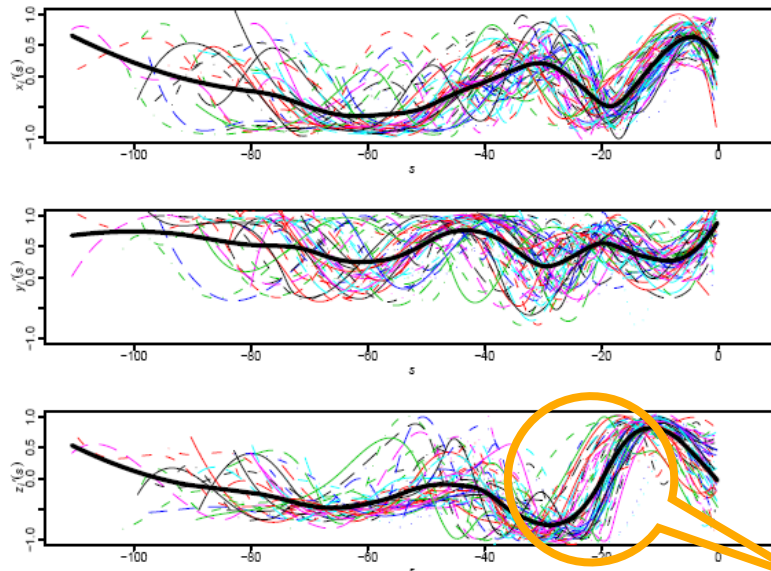
Curvature function



$$C_i(s) = \frac{\|(x'_i(s) \ y'_i(s) \ z'_i(s)) \times (x''_i(s) \ y''_i(s) \ z''_i(s))\|}{\|(x'_i(s) \ y'_i(s) \ z'_i(s))\|^3}$$

Sangalli, Secchi, Vantini, Veneziani, 2009; Sangalli, Secchi, Vantini, Vitelli, 2010

Centerline first derivatives



Phase Topological Theory for Alignment:
Vaastanga (2012)
(dependent on dimensions of
body structure and arteries)

- To enable meaningful comparisons across patients we need to decouple between-patients *phase variability* and between-patients *amplitude variability*
 - due to *differences in the dimensions* of patients carotids
 - due to *differences in the morphological shapes* of patients carotids

Data Registration

Similarity Index between Curves

$$\rho(\mathbf{c}_i, \mathbf{c}_j) = \frac{1}{3} \cdot [\rho(x_i, x_j) + \rho(y_i, y_j) + \rho(z_i, z_j)]$$

Group of Warping Functions

$$W = \{h : h(s) = ms + p \text{ with } m \in \mathbb{R}^+, p \in \mathbb{R}\}$$



- ✓ $\rho(x_i, x_j) = \frac{\int_{S_{ii}} x'_i(s)x'_j(s)ds}{\sqrt{\int_{S_{ii}} x'_i(s)^2 ds} \sqrt{\int_{S_{ii}} x'_j(s)^2 ds}}$
 - ✓ $|\rho(\mathbf{c}_i, \mathbf{c}_j)| \leq 1$
 - ✓ $\rho(\mathbf{c}_i, \mathbf{c}_j) = 1 \Leftrightarrow \exists \mathbf{A} \in (\mathbb{R}^+)^3, \mathbf{B} \in \mathbb{R}^3 : \begin{cases} x_i = A_x x_j + B_x \\ y_i = A_y y_j + B_y \\ z_i = A_z z_j + B_z \end{cases}$
 - ✓ $\rho(\mathbf{c}_i, \mathbf{c}_j) = \rho(\mathbf{c}_i \circ h, \mathbf{c}_j \circ h) \quad \forall h \in W$
 - ✓ $\rho(\mathbf{c}_i \circ h, \mathbf{c}_j) = \rho(\mathbf{c}_i, \mathbf{c}_j \circ h^{-1}) \quad \forall h \in W$
- $$\sup_{h \in W} \rho(\mathbf{c}_i \circ h, \mathbf{c}_j) = \sup_{h \in W} \rho(\mathbf{c}_i, \mathbf{c}_j \circ h)$$

Similarity index considers similar what doctors consider similar

W-invariance of similarity index
Isometry of W action
Parallel orbit property

Data Registration

Iterative Registration Algorithm

Unregistered Derivatives



Estimate
reference first derivatives $x_0'(t), y_0'(t), z_0'(t)$

Loess with Gaussian Kernel and span = 0.15 on the 65 patients



For each patient, find h_i that maximizes similarity between
reference derivatives $x_0'(t), y_0'(t), z_0'(t)$
and patient derivatives $x_i'(h_i^{-1}(t)), y_i'(h_i^{-1}(t)), z_i'(h_i^{-1}(t))$

For each patient look for the affine transformation of the abscissa maximizing

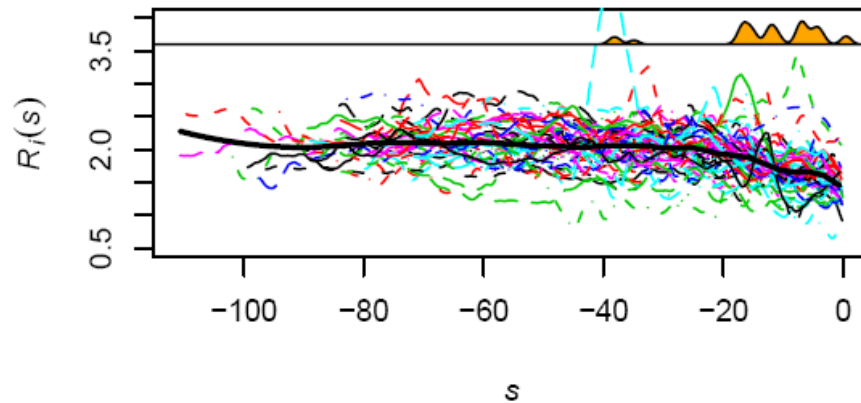
$$\frac{1}{3} \left[\frac{\int_{T_i} x_i'(h_i^{-1}(t))x_0'(t)dt}{\sqrt{\int_{T_i} x_i'(h_i^{-1}(t))^2 dt} \sqrt{\int_{T_i} x_0'(t)^2 dt}} + \frac{\int_{T_i} y_i'(h_i^{-1}(t))y_0'(t)dt}{\sqrt{\int_{T_i} y_i'(h_i^{-1}(t))^2 dt} \sqrt{\int_{T_i} y_0'(t)^2 dt}} + \frac{\int_{T_i} z_i'(h_i^{-1}(t))z_0'(t)dt}{\sqrt{\int_{T_i} z_i'(h_i^{-1}(t))^2 dt} \sqrt{\int_{T_i} z_0'(t)^2 dt}} \right]$$



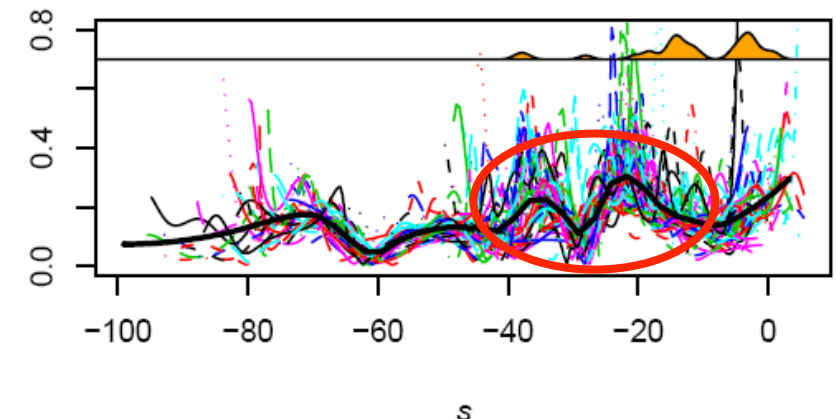
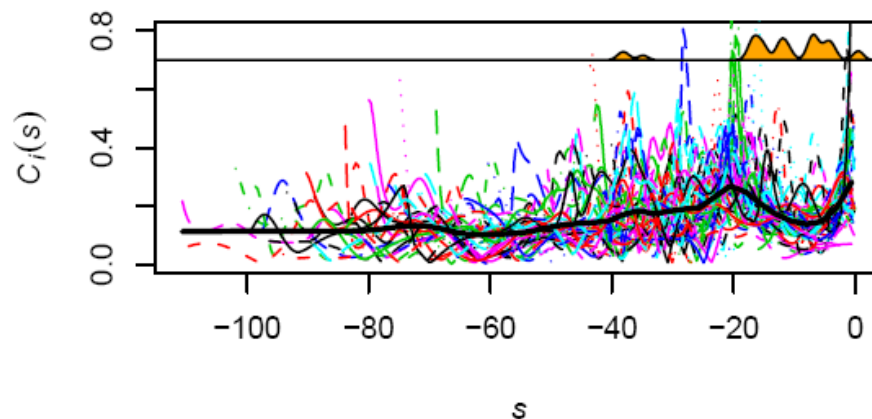
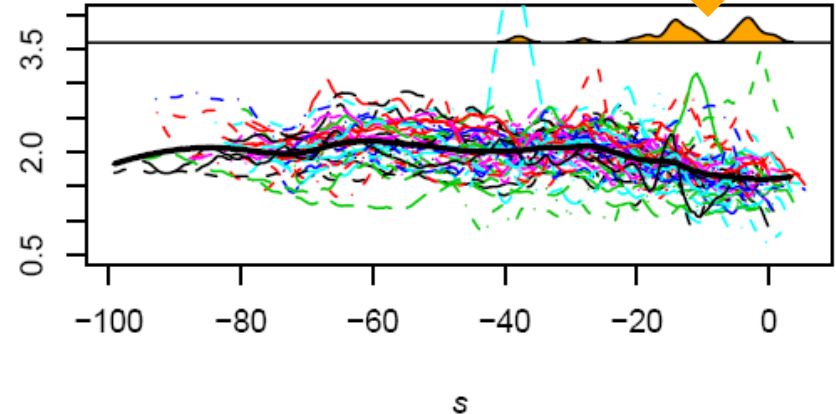
Registered Derivatives and Warping Functions

Data Registration

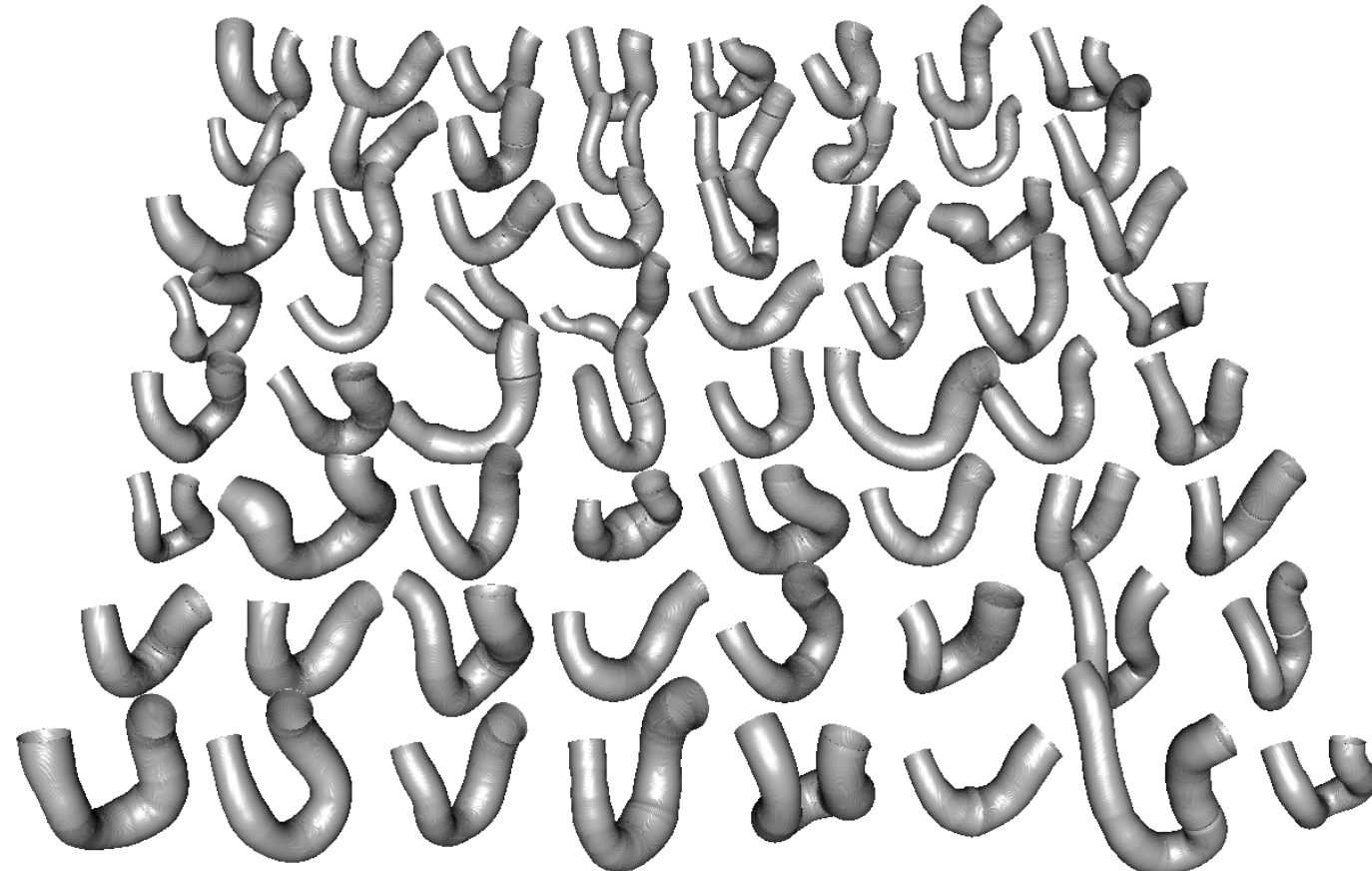
Unregistered
Radius and Curvature Profiles



Registered
Radius and Curvature profiles



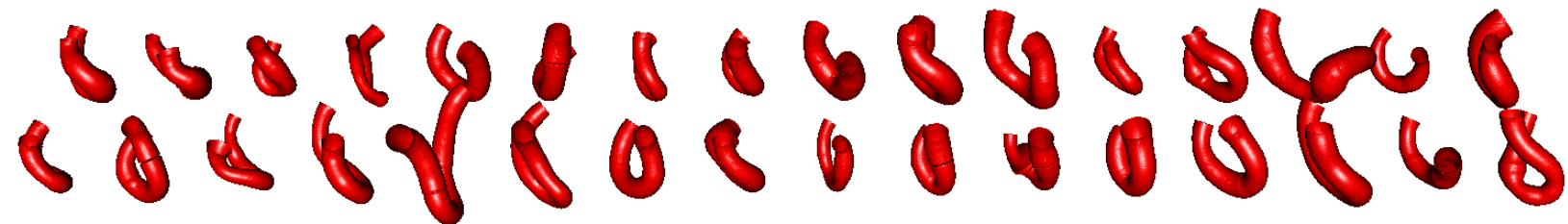
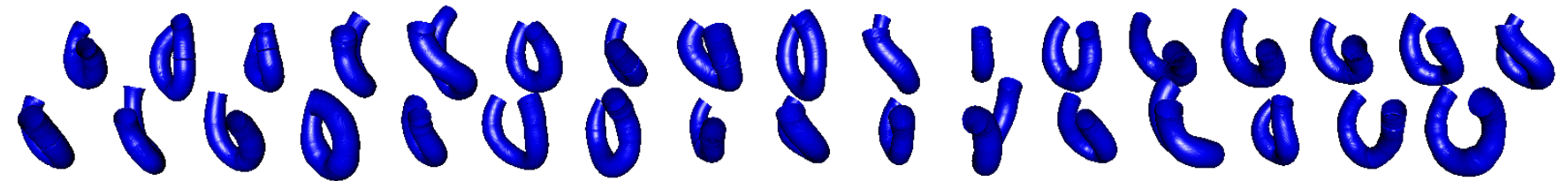
The sample of 65 ICA: each patient is represented by the **REGISTERED** centerline and radius of ICA



We want to use vessel radius and curvature to discriminate:

Aneurysm at or after ICA bifurcation

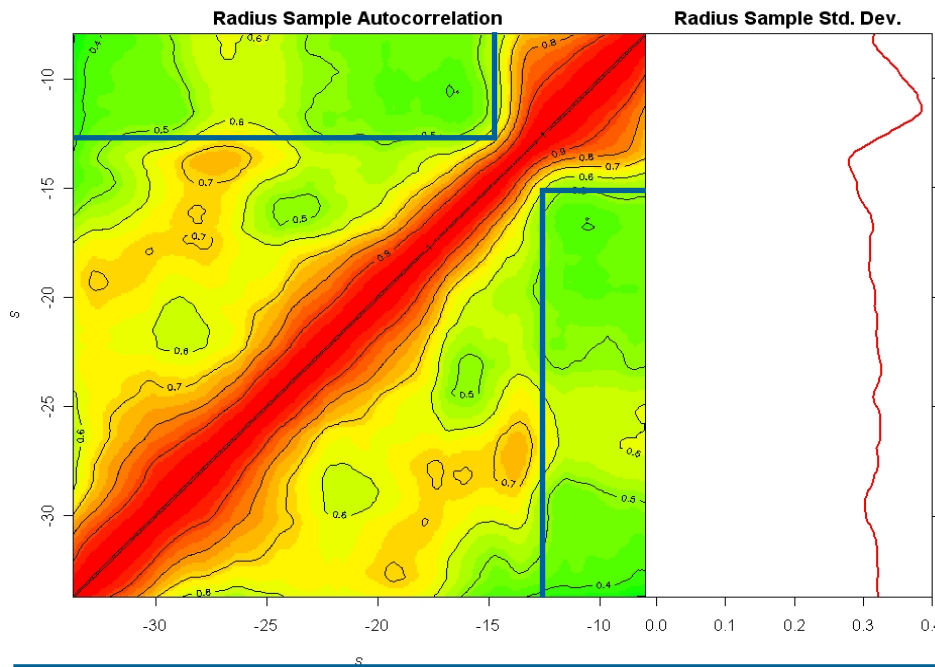
Upper Group: 33



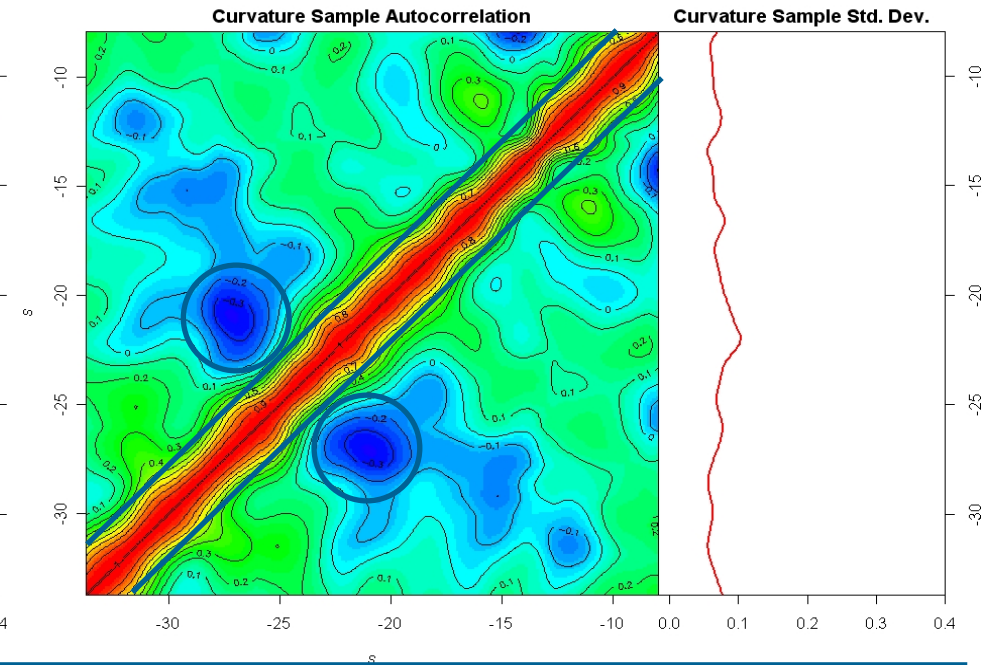
Lower Group: 32

Aneurysm before ICA bifurcation or no aneurysm

Sample Autocorrelation Function
and Std. Dev. for Radius Profiles
of aligned centerlines



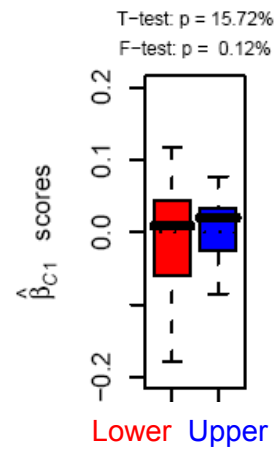
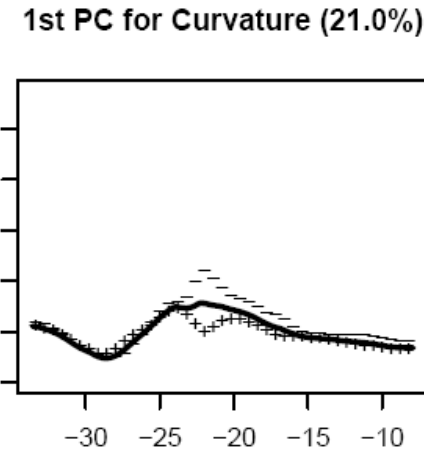
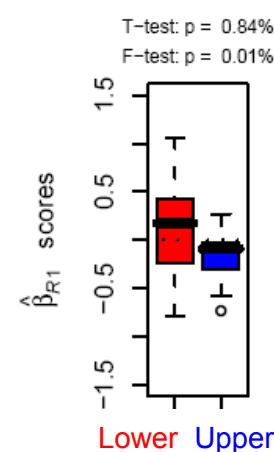
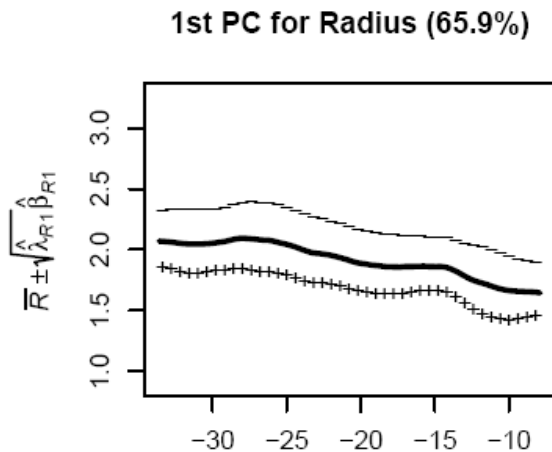
Sample Autocorrelation Function
and Std. Dev. for Curvature Profiles
of aligned centerlines



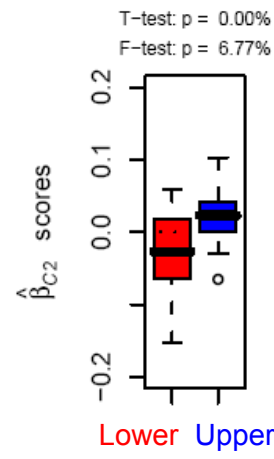
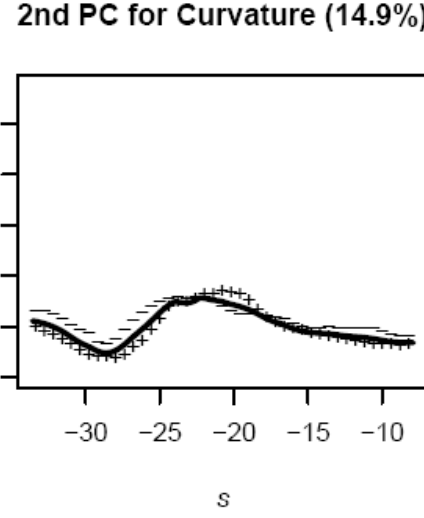
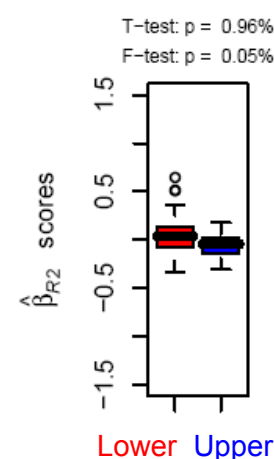
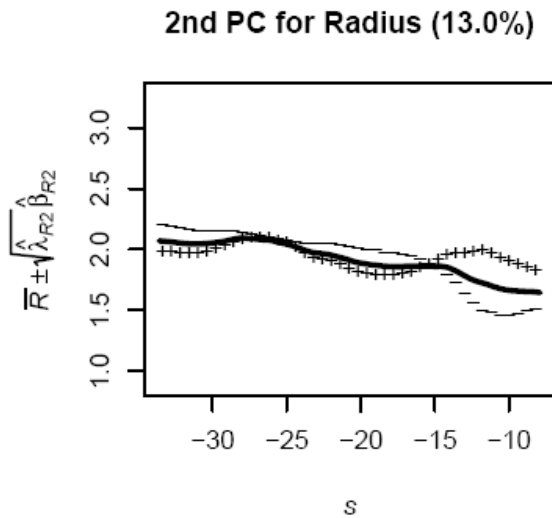
First step: dimension reduction through spectral decomposition of radius and curvature sample autocovariance functions (Functional Principal Component Analysis)
Second step: quadratic discriminant analysis on relevant scores

Functional Principal Component Analysis

(Sangalli, Secchi, Vantini, Veneziani, 2009)

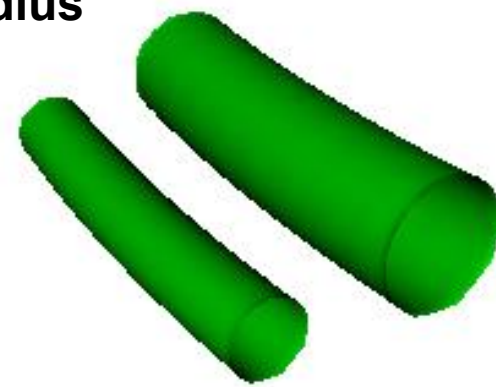


Lower Group - Upper Group

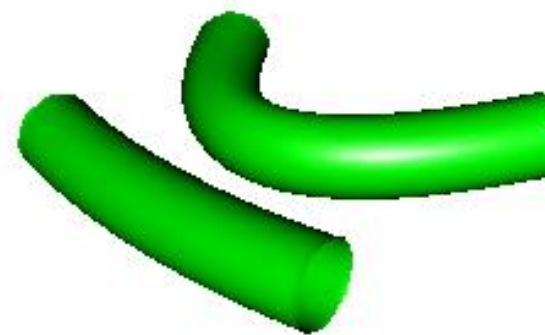


FPCA of the Aneurisk data

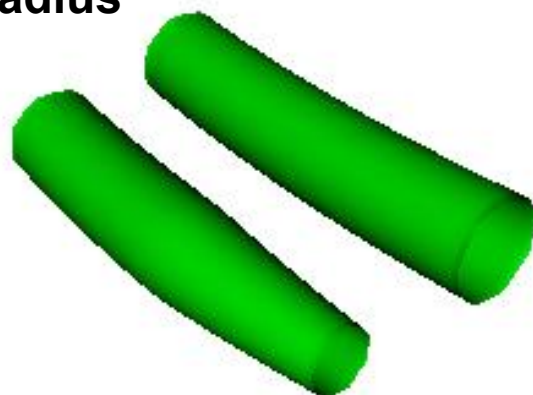
**1st PC
Radius**



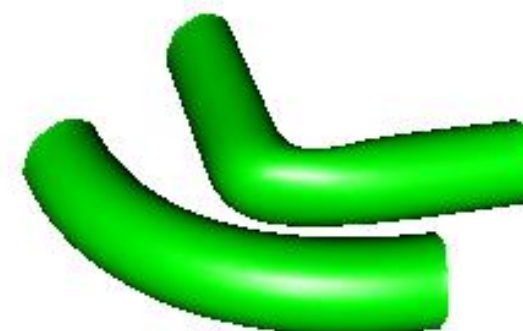
**1st PC
Curvature**



**2nd PC
Radius**

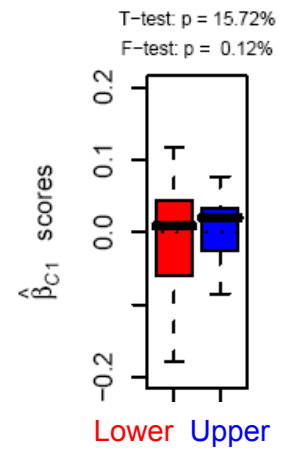
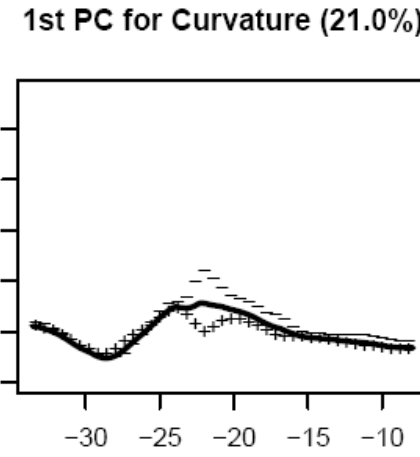
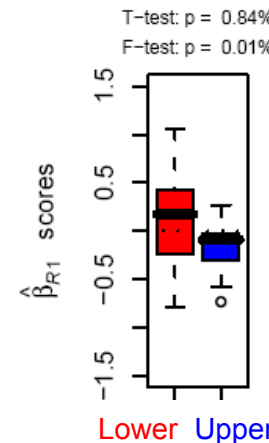
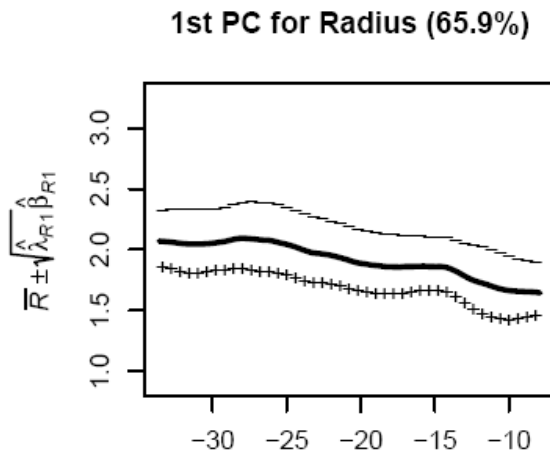


**2nd PC
Curvature**

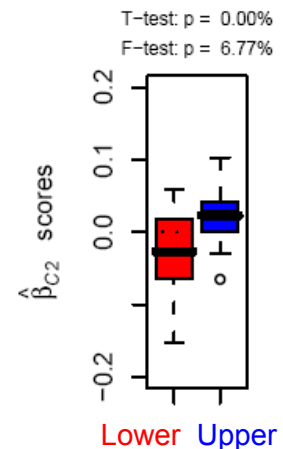
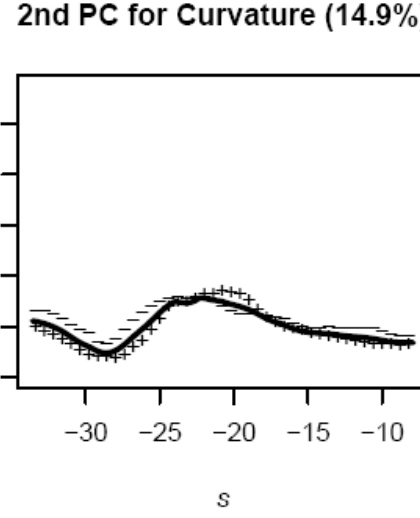
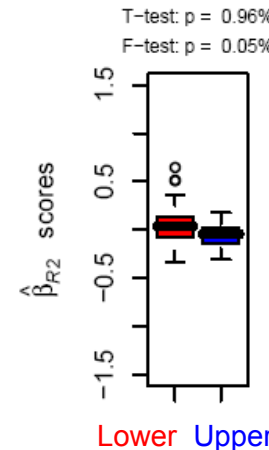
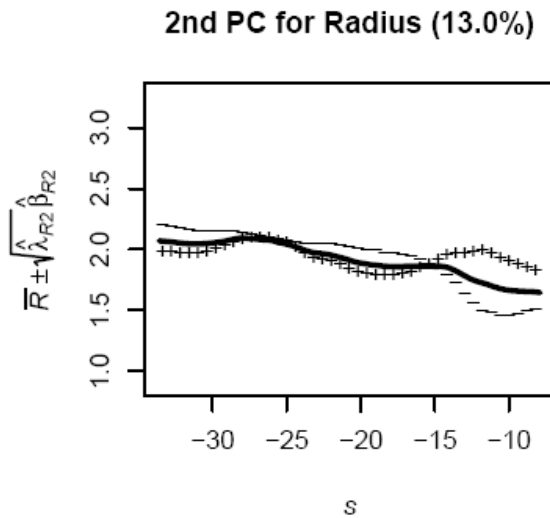


Functional Principal Component Analysis

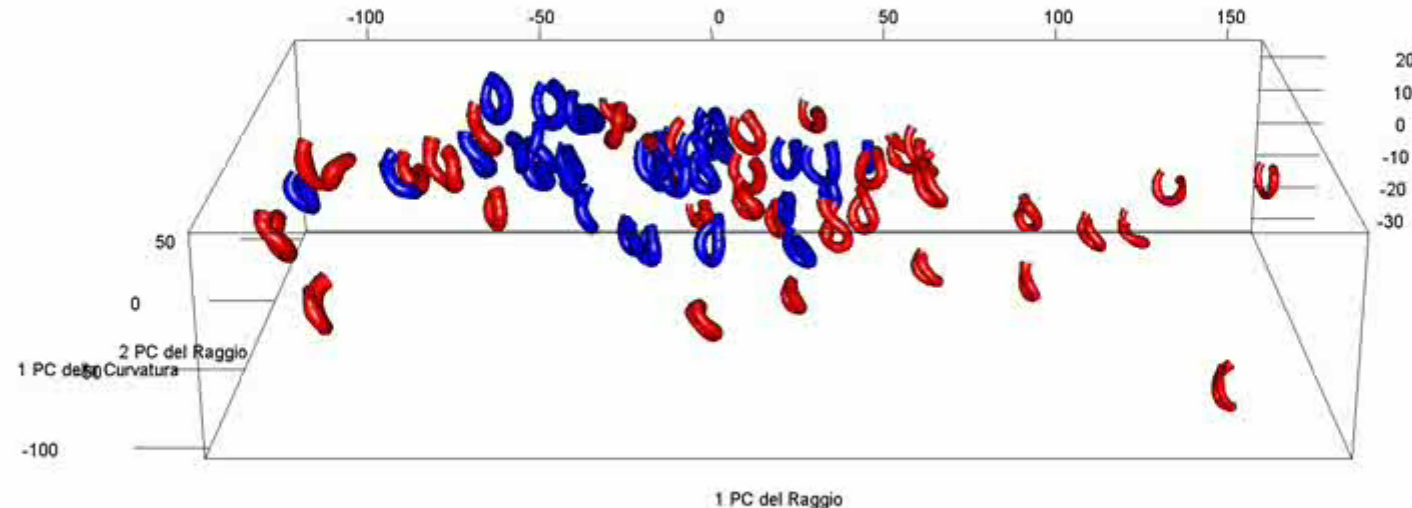
(Sangalli, Secchi, Vantini, Veneziani, 2009)



Lower Group - Upper Group

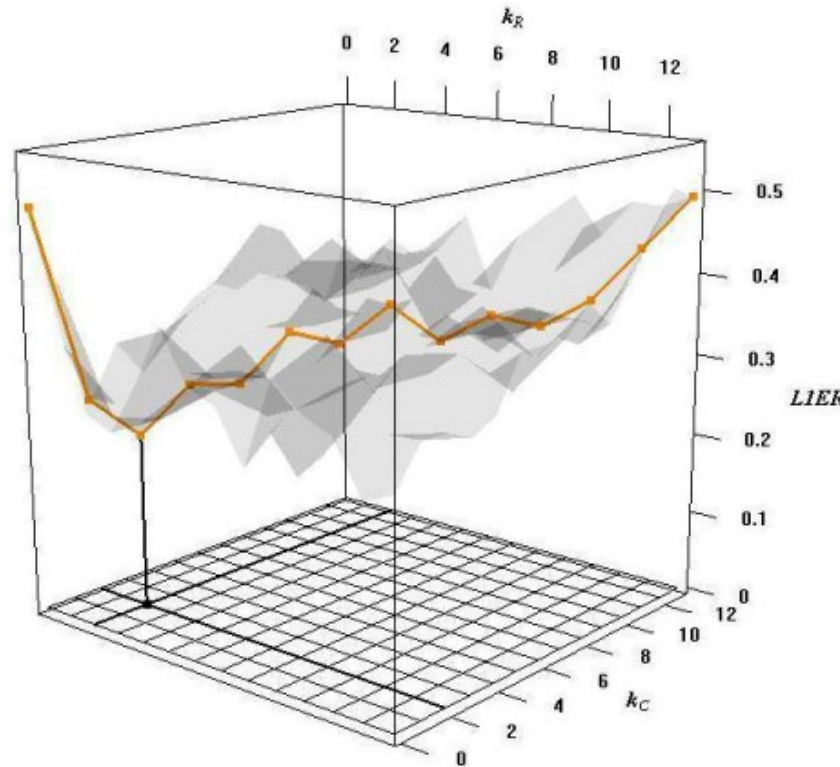


Dimension reduction: Functional Principal Component Analysis



Representation of the 65 ICA in the space generated by:
2 PC of radius and 1 PC of curvature

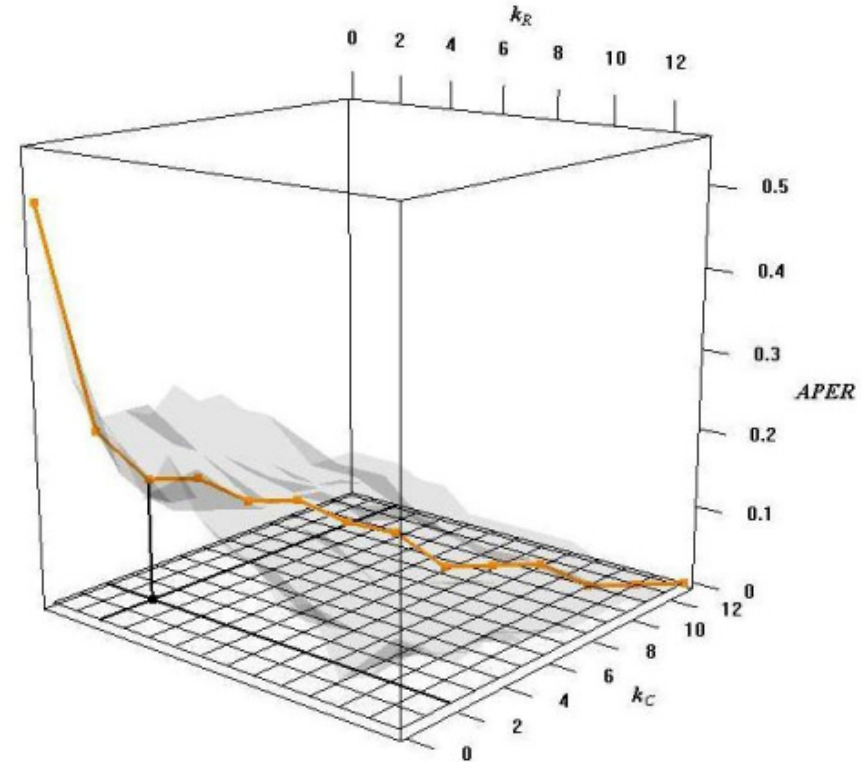
Quadratic Discriminant Analysis of Functional PCA scores



L1ER = 21.5%

	Lower	Upper
Predicted	Predicted	Predicted
Lower	23	9
Upper	5	28

	Lower	Upper
Predicted	Predicted	Predicted
Lower	35.4%	13.8%
Upper	7.7%	43.1%



APER = 16.9%

	Lower	Upper
Predicted	Predicted	Predicted
Lower	23	9
Upper	2	31

	Lower	Upper
Predicted	Predicted	Predicted
Lower	35.4%	13.8%
Upper	3.1%	47.7%

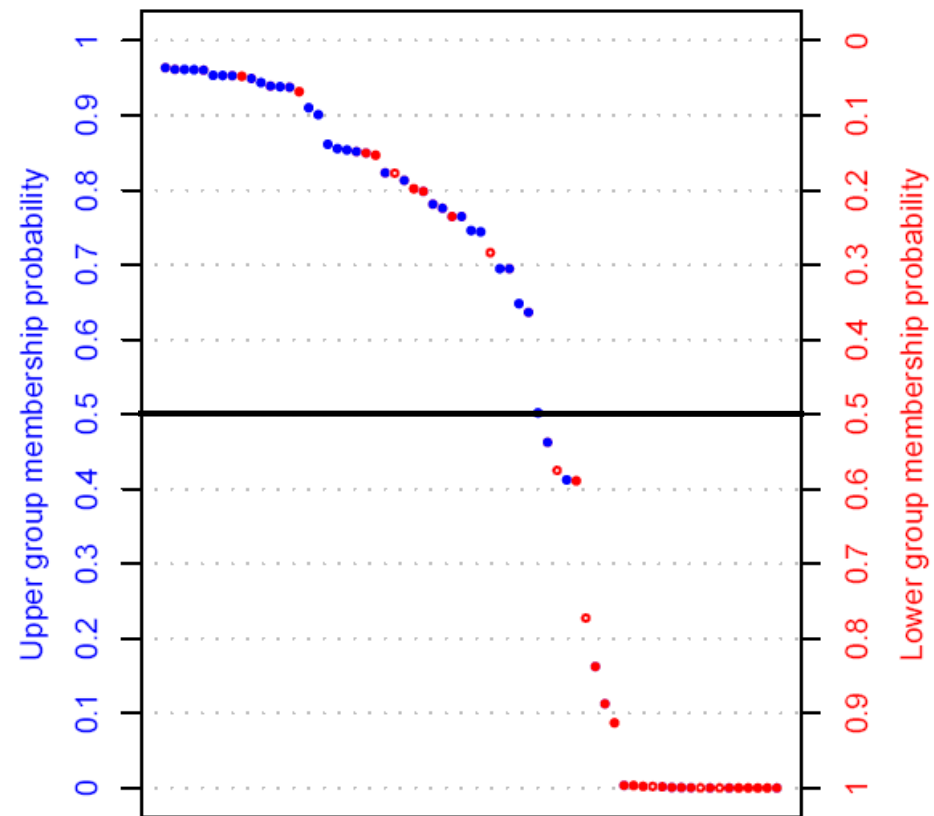
Discriminant analysis of functional principal component scores

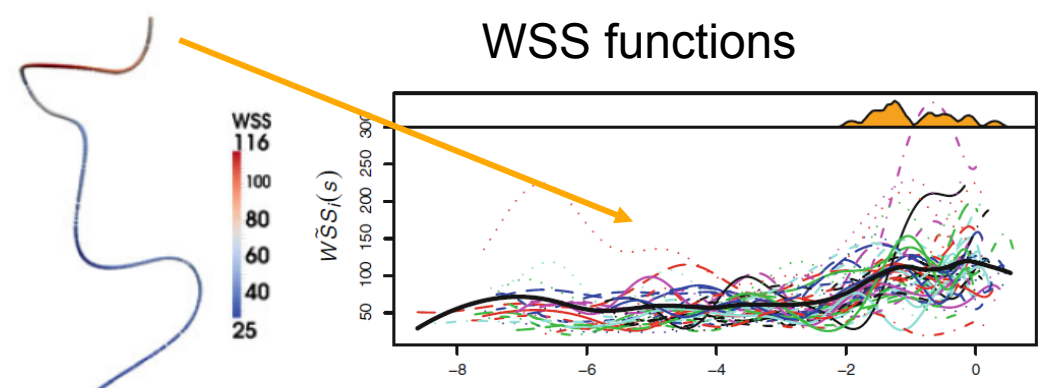
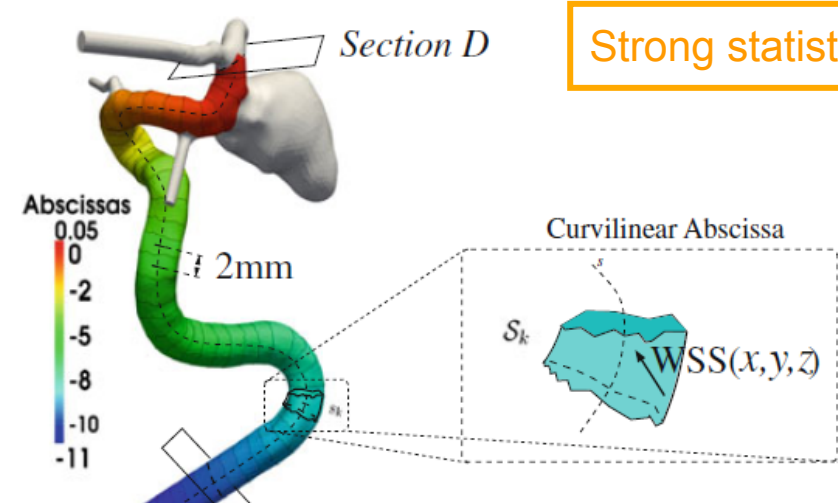
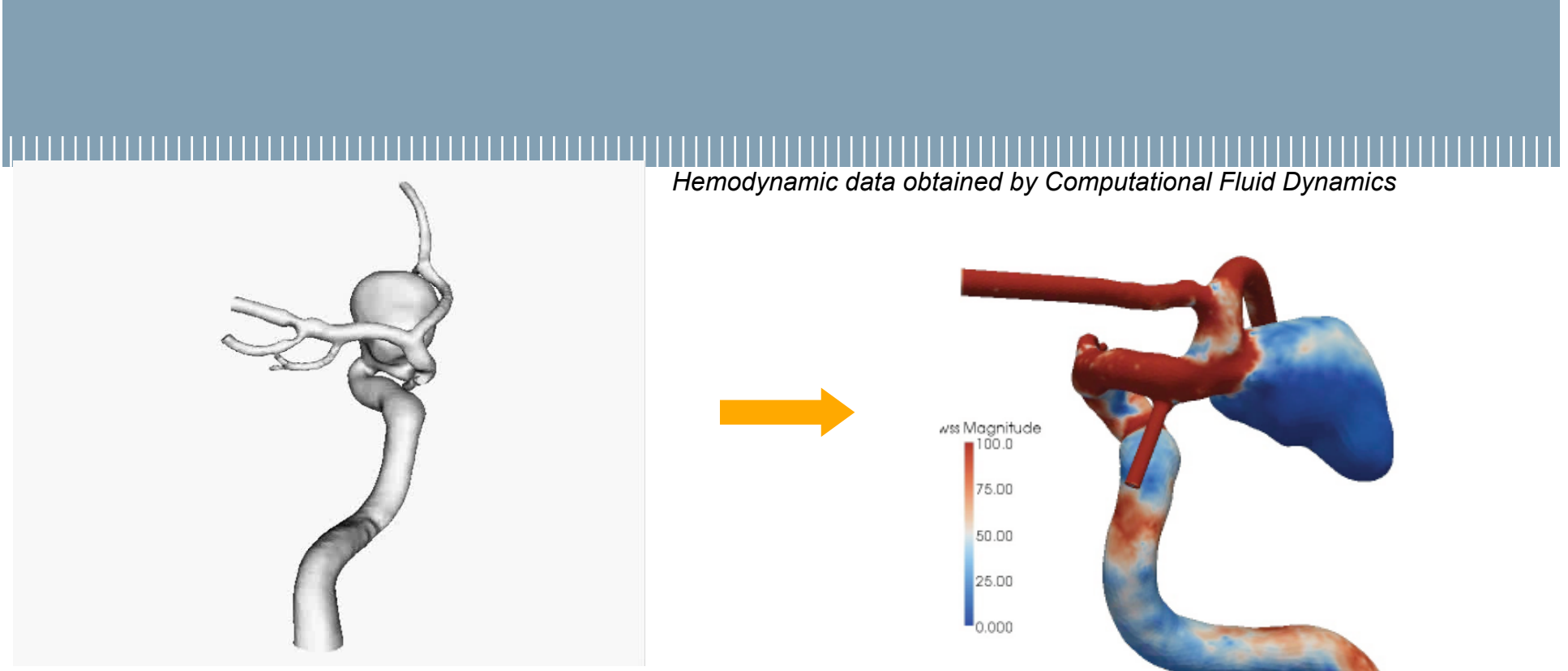
23

→ **Upper group** patients are very well characterized by this two geometric features

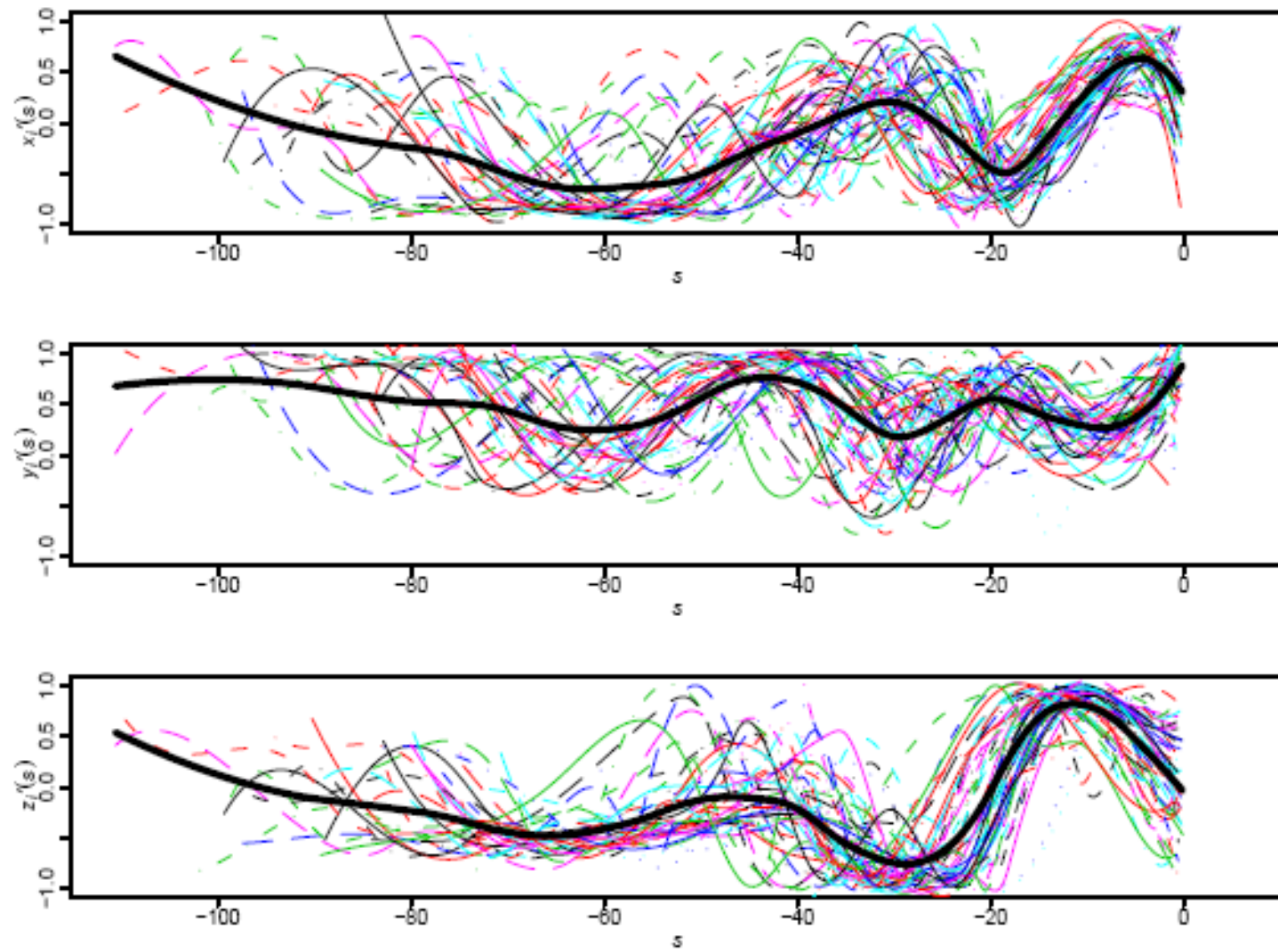
A quadratic discriminant analysis of scores correctly identifies 31 out of the 33 patients in this group

- Large vessels
- Strong tapering
- High within-patient curvature variability, presence of straight tracts and elbows
- Low between-patient curvature and radius variability

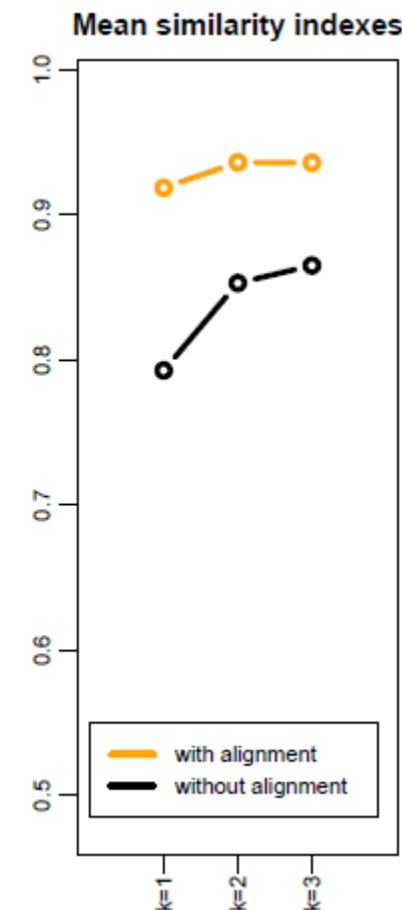
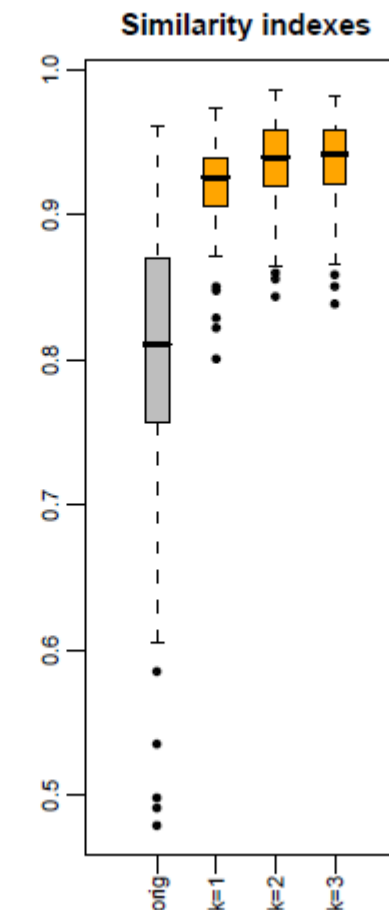
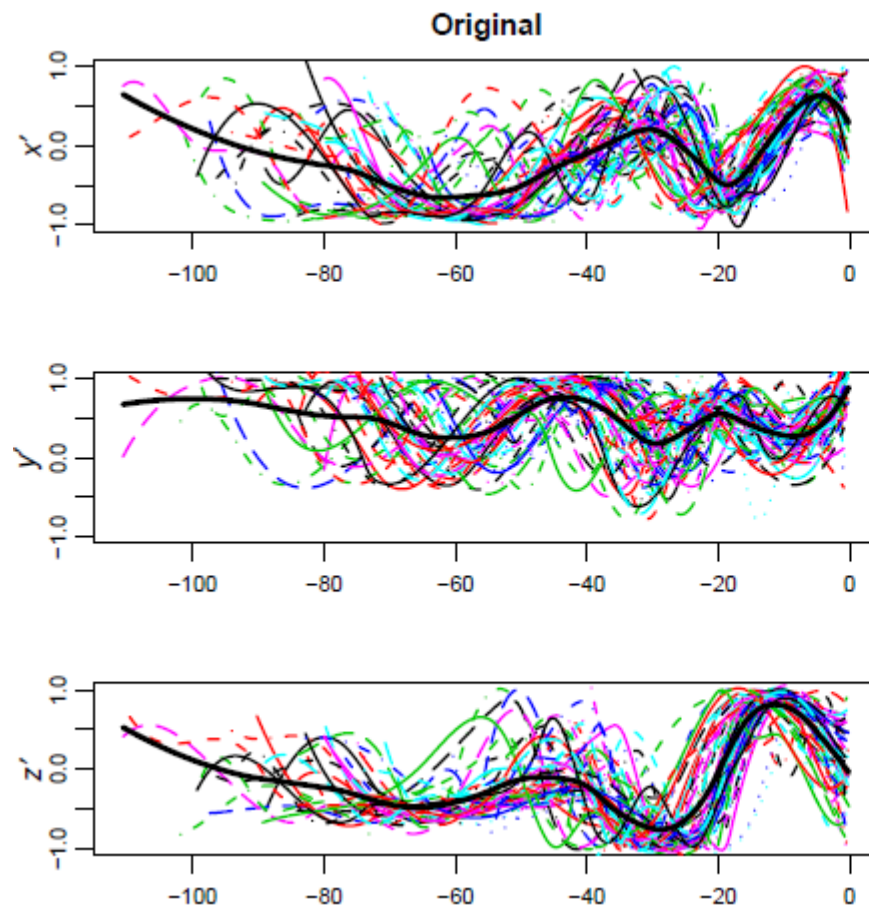




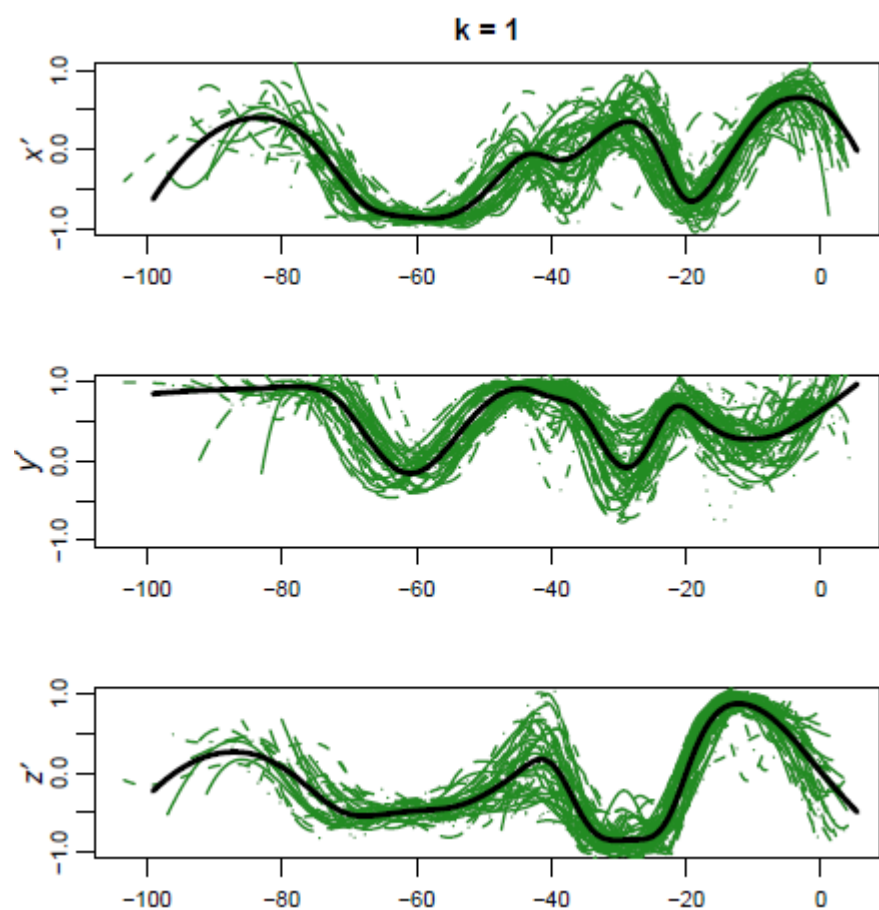
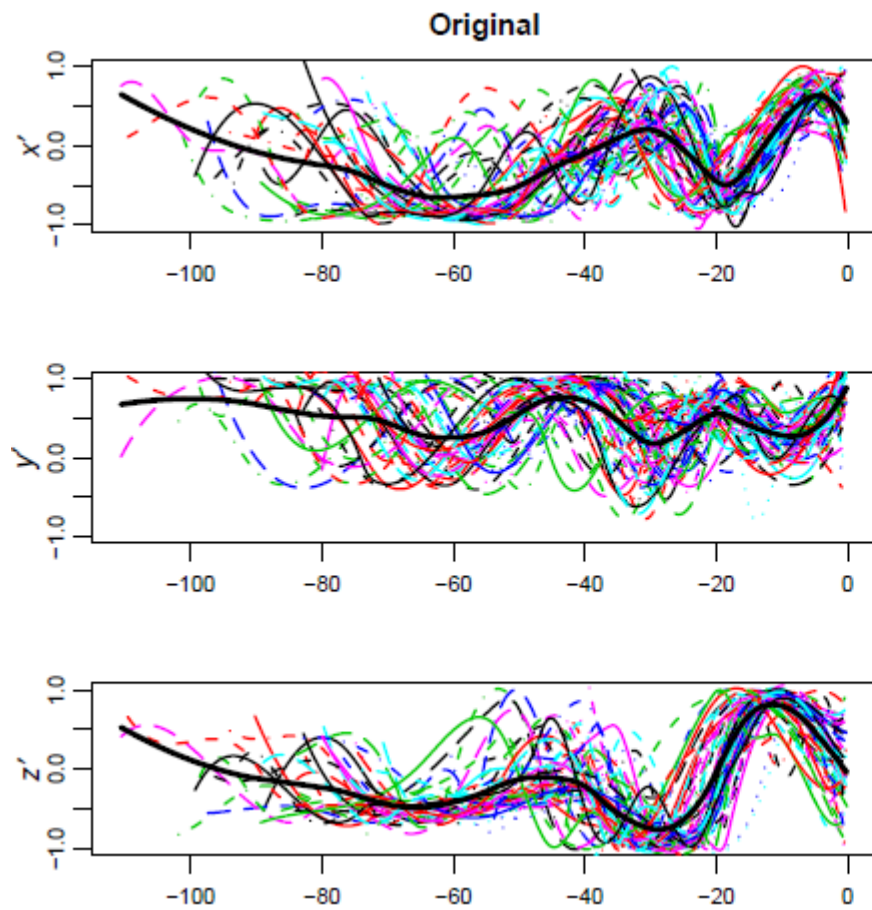
ICA centerlines first derivatives



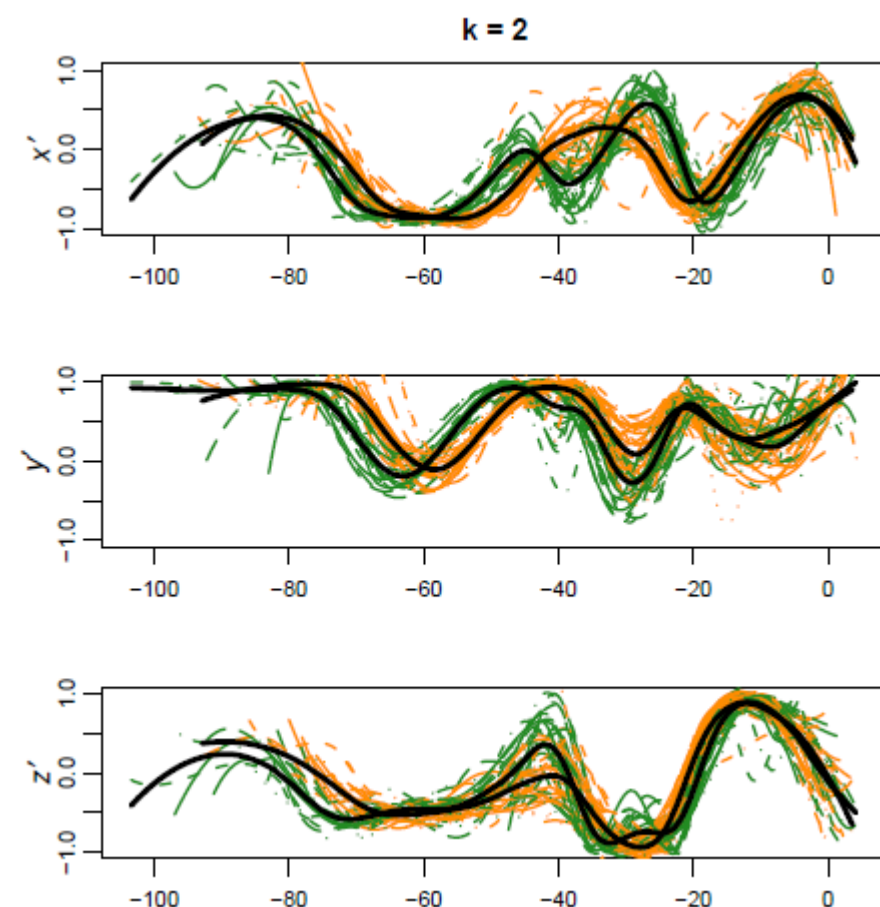
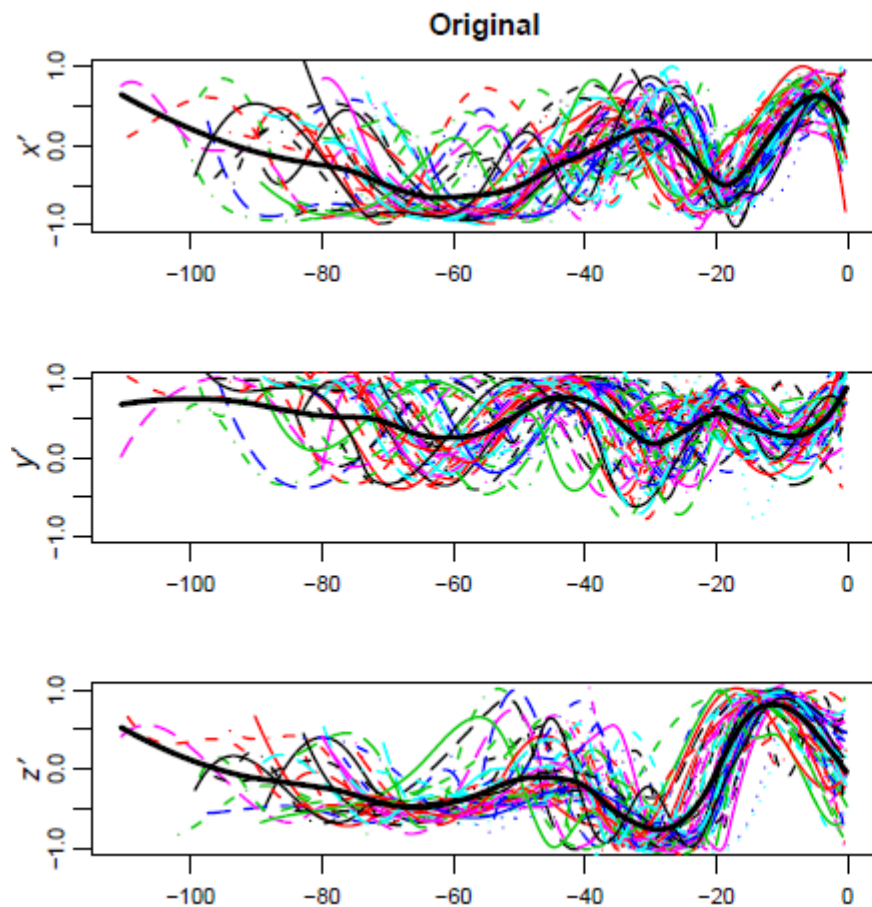
K-mean Alignment Performances



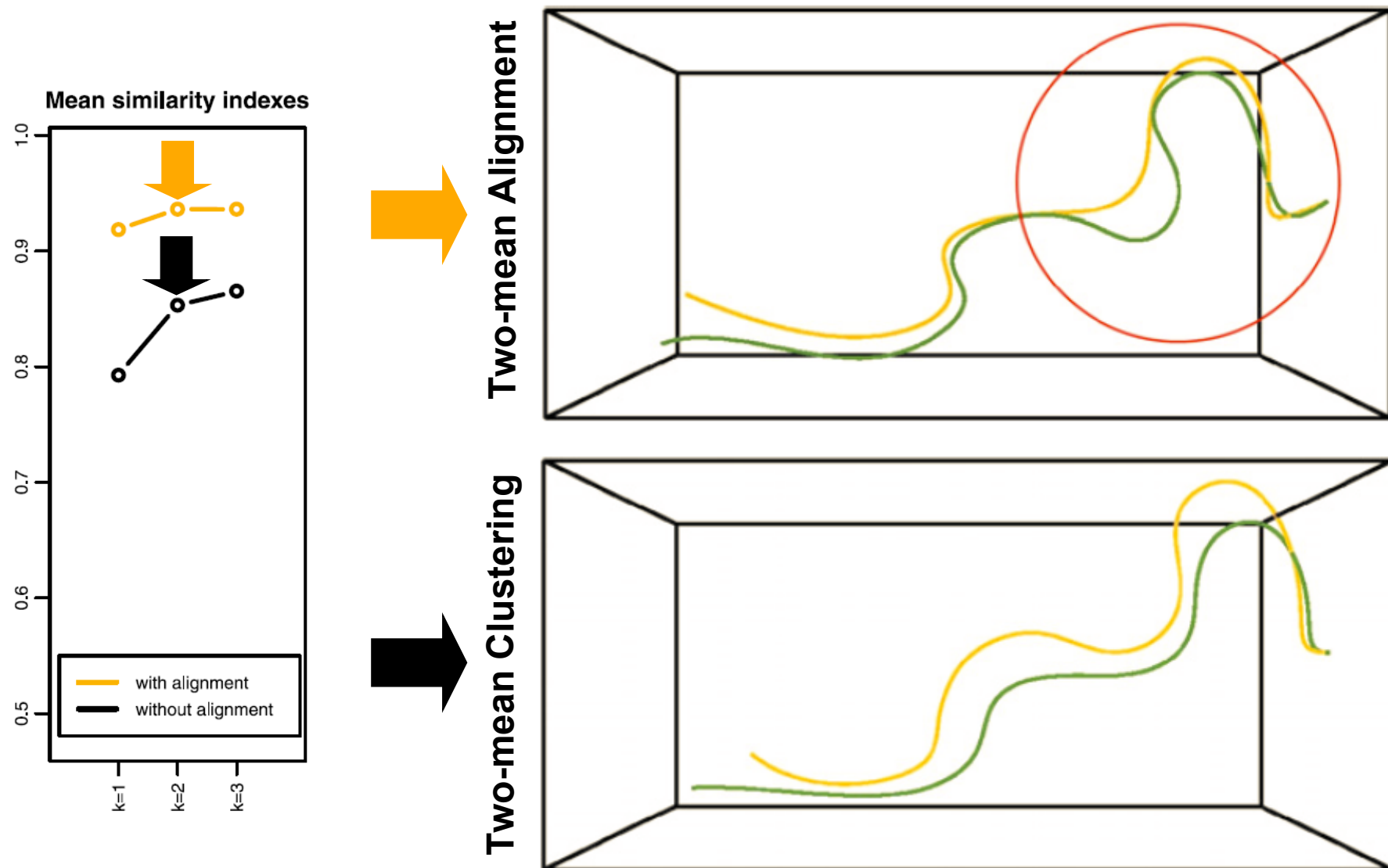
One-mean Alignment



Two-mean Alignment

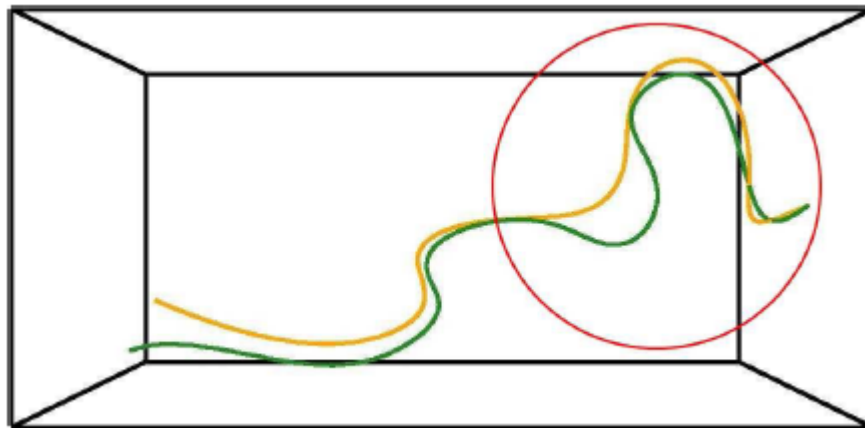


Two-mean Alignment vs Two-mean Clustering



Clustering

Two-mean Alignment



Clusters that are
morphologically different

30 S-shaped ICAs
vs
35 Ω-shaped ICAs

Krayenbuehl et al. (1982)

	No Aneurysm	Aneurysm along ICA	Aneurysm downstream ICA
S-shaped ICAs	100%	52%	30%
Ω-shaped ICAs	0%	48%	70%

P-value of Pearson's Chi-squared test for independence equal to 0.0013



Fluid-dynamical interpretation of the onset of cerebral aneurysms